Adsorption of Methylene Blue onto Hydrophobic Activated Carbon

Said M. Al-Mashaikhi, El-Said I. EL-Shafey*, Saleh Al-Busafi, FakhrEldin O. Suliman

Department of Chemistry, College of Science, Sultan Qaboos University, P.O. 36, Al-Khod 123, Muscat, Sultanate of Oman. *Email: elshafey@squ.edu.om.

ABSTRACT: Activated carbon (AC) was prepared from date palm leaflets using NaOH activation. AC was oxidized using concentrated HNO_3 to produce oxidized activated carbon (ON). Alkylamines including methylamine (M), dimethylamine (DM), ethylamine (E), diethylamine (DE), and diisopropylamine (DIP) were covalently immobilized onto ON to produce ONM, ONDM, ONE, ONDE, and ONDIP hydrophobic activated carbons, respectively. The surface area of AC (588 m^2/g) decreased on oxidation with a further decrease on functionalization. These carbons were tested for methylene blue (MB) adsorption. An initial pH 7 was found to be optimum for the adsorption of MB. The hydrophobic activated carbons showed faster adsorption (except for ONDE), than AC with adsorption data following a pseudo-second-order kinetic model. The rate of adsorption increased with increasing temperature. The activation energy, E_a, was less than 42 kJ/mol indicating physical adsorption. Equilibrium adsorption follows an L-type isotherm with the adsorption data following the Langmuir model. The adsorption capacity of MB follows the order of ONDIP > ONE > ONDM > AC > ON > ONM > ONDE. Thermodynamic parameters indicate spontaneous and endothermic adsorption. Carbon reuse for MB adsorption was more efficient for ONDIP, ONE, and ONDM than AC.

Keywords: Activated carbon; Methylene blue; Alkylamine; Hydrophobic; Adsorption.

<div dir="rtl">

امتزاز المثيليين الأزرق على الكربون النشط الكاره للماء

سعيد المشايخي، السعيد الشافعي ، صالح البوصافي، فخر الدين سليمان

الملخص: تم تحضير الكربون المنشط (AC) من وريقات نخيل التمر باستخدام تنشيط هيدروكسيد الصوديوم. وتم أكسدة الكربون المنشط باستخدام حمض النيتريك المركز لإنتاج الكربون المؤكسد (ON). تم تثبيت أمينات الألكيل لإنتاج الكربون الكاه للماء بما في ذلك ميثيل أمين (M) ، وثنائي ميثيل أمين (DM)، وإيثيل أمين (E) ، وثنائي إيثيل أمين (DE) ، وثنائي أيزوبروبيل أمين (DIP) تساهميًا لإنتاج ONM ، و ONDM ، و ONE ، و ONDE ، و ONDIP ل علي التوالي. وتبين أن مساحة السطح للكربون النشط (588 متر2/جرام) قد انخفضت بالأكسدة وانخفضت أكثر مع تثبيت الألكيل أمين. وتم اختبار الكربونات الناتج لازالة الميثيلين الأزرق .ووجد أن الرقم الهيدروجيني الأولي 7 هو الأمثل لامتزاز الميثيلين الأزرق. تُظهر الكربونات المنشطة الكارهة للماء امتزازاً أسرع للميثيلين الأزرق باستثناء (ONDE) من AC مع اتباع بيانات الامتزاز النموذج الحركي من الدرجة الثانية. وقد زاد معدل الامتزاز مع ارتفاع درجة الحرارة. وتبين أن طاقة التنشيط أقل من 42 كيلو جول / مول مما يشير إلى الامتزاز الفيزيائي. يتبع امتزاز الإتزان النوع L واتباع بيانات الامتزاز لنموذج لانجمير.ووجد أن سعة امتزاز الميثيلين الأزرق تتبع الترتيب : <ONM <ON <AC <ONDM <ONE <ONDIP ONDE. وتشير دراسة الديناميكية الحرارية إلى امتزاز تلقائي وماص للحرارة. أظهرت دراسة تدوير الكربون امتزازا أسرع وأكثر لـ ONDIP و ONE وONDM مقارنةً بالكربون المنشط.

الكلمات المفتاحية: الكربون النشط ـ الكاره للمياه ـ الميثيلين الازرق ـ الكيل أمين ـ إمتزاز

</div>

ADSORPTION OF METHYLENE BLUE ONTO HYDROPHOBIC ACTIVATED CARBON

1. Introduction

Dyes are toxic pollutants and can cause a threat to aquatic organisms and human health. Recent data shows that there are more than 100,000 commercial dyes, with an annual production of over 70,000 tonnes/year [1,2]. The textile industry utilizes more than 10,000 tonnes of dyes every year from which 100 tonnes are discharged into the environment [2,3]. Most of these dyes are toxic to the aquatic environment. Their complex chemical structures make them resistant to degradation by light, heat, and oxidizing agents, increasing the danger of this type of chemicals [4-6]. The toxicity of azo dyes arises from the presence of amines, while the color of anthraquinone dyes remains in effluents for a long time as they are resistant to degradation. In addition, the high solubility of reactive dyes and their chemical stability in water causes serious problems for the aquatic environment [7]. In aquatic ecosystems, photosynthetic activity is affected by decreasing light penetration [2]. Moreover, these harmful materials are carcinogenic to various fish species. Dyes can cause damage to human health and reduce the effectiveness of the reproductive system, kidneys, brain, liver, and central nervous system [6, 8].

Typical methods used for the removal of dyes from water include ozonation [9], photocatalytic degradation [10,11], advanced oxidation [12], microbial biodegradation [13], coagulation and flocculation [14], filtration and membrane-filtration processes [15]. Such methods have the essential limitations of being complex and uneconomic [16]. Adsorption has proven superior to other techniques in terms of flexibility, simplicity of design, and initial cost [17]. In previous studies activated carbon prepared from pepper stems showed an adsorption capacity of 174 mg/g with the best performance at pH 8.0 [18] and activated carbon prepared from date palm leaves using KOH activation showed 270 mg/g, while after ethylamine functionalization the capacity increased to 393 mg/g with best performance at pH 7 [19]. Dehydrated carbon at pH 7 had a capacity of 196 mg/g, and after functionalization using ethylamine showed 296 mg/g [20]. Other adsorbents have also been used including clay [21], zeolite [22], bentonite [6], and biosorbents [23]. In this study, AC was prepared from date palm leaflets using NaOH activation. AC was oxidized, using nitric acid, and was surface functionalized using alkylamines with different sizes of the alkyl groups via amide coupling to produce hydrophobic activated carbons. These carbons were tested for the removal of methylene blue (MB) from the aqueous solution in terms of kinetics and equilibrium. The effect of the different sizes of alkyl amines on the extent of functionalization and its performance towards methylene blue adsorption is a novel area of study and is discussed in this paper.

2. Materials and methods

2.1 Materials

The chemicals used were of analytical grade. Activated carbon (AC) was prepared from clean dried date palm leaves using NaOH activation. AC was oxidized using concentrated nitric acid at 80 ^{o}C to produce oxidized activated carbon (ON). ON was covalently functionalized using methylamine (M), dimethylamine (DM), ethylamine (E), diethylamine (DE), and diisopropylamine (DIP) via amide coupling to produce the hydrophobic activated carbons: ONM, ONDM, ONE, ONDE, and ONDIP, respectively. The study of AC preparation, surface functionalization, and characterization was carried out in our laboratories, and published previously [24]. The stock solution of methylene blue (MB) (1000 mg/L) was prepared in deionized water. The standards and adsorption test solutions were prepared by suitable dilution in deionized water.

2.1 Effect of pH on MB adsorption

To investigate the effect of pH on MB adsorption, ~ 0.06 g of carbon was mixed with 25 mL of MB solution (100 mg/L) in clean glass vials at different initial pH values of 3.0-9.0. Before the addition of the pre-weighed adsorbent, the pH was adjusted using a few drops of dilute NaOH or HCl. At 20 ^{o}C, the samples were shaken regularly until equilibrium was reached. Residual MB was analyzed using a Varian/Cary/50 Conc UV-Visible spectrophotometer at λ_{max} 665 nm with deionized water as blank. For all carbons, initial pH 7 was found optimal for MB adsorption and, thus, was selected for the kinetic, equilibrium, and carbon recycle studies of MB adsorption.

2.2 Kinetics of MB adsorption

In the kinetic experiments, 0.12 g of carbon was mixed with 50 mL of MB solution (100 mg/L) at initial pH of 7. The adsorption vessels were shaken mechanically for 48 hours. At different time intervals, aliquots of supernatant were withdrawn and analyzed. The kinetic experiments were carried out at 20 and 40 ^{o}C.

2.3 Equilibrium adsorption

The equilibrium studies were carried out by mixing ~ 0.06 g of carbon with 25 mL of MB solution (50 – 1000 mg/L) at initial pH 7 at two temperatures of 20 and 40 ^{o}C. The adsorption vessels were kept under mechanical agitation until equilibrium was reached. Residual MB was withdrawn and analyzed.

2.4 Adsorbent recycle

For MB recovery, 0.12 g of carbon was added to 50 mL of MB solution (100 ppm) at initial pH 7 and was kept for 48 hours under agitation until equilibrium was reached. After equilibrium, samples were separated for analysis. The adsorbent was washed with a boiling solution of sodium hydroxide at pH 10 followed by deionized water. The samples were washed with dilute HCl to neutralize residual NaOH, followed by deionized water until the adsorbent was acid-free. The carbon was partially dried and transferred carefully to a new adsorption vessel containing 50 mL of MB solution under the same conditions as the first adsorption cycle (100 ppm, pH 7). The adsorption mixture was left under agitation until equilibrium was reached and samples of MB were separated for analysis. Residual MB concentration was determined using a Varian/Cary/50 Conc UV-visible spectrophotometer at λ_{max} of 665 nm with deionized water as blank. All the experiments and analysis were carried out at least twice.

3. Results and discussion

The study of AC preparation, surface oxidation, and functionalization using different alkylamines was carried out in our laboratories and published elsewhere, and included the carbons tested in this study [24]. A schematic representation of the seven carbons under investigation is presented in Figure 1. Fourier transform infrared (FTIR), carbon, hydrogen, and nitrogen analysis (CHN), and thermogravimetric analysis (TGA) showed that surface functionalization was successful [24]. The surface areas for the carbons were 588, 259.3, 217.6, 150.3, 108.8, 93.2, and 72.0 for AC, ON, ONM, ONDM, ONE, ONDE, and ONDIP, respectively. The extent of functionalization followed the order ONM > ONDM > ONE > ONDE > ONDIP [24] that corresponds to the size of the alkylamine immobilized.
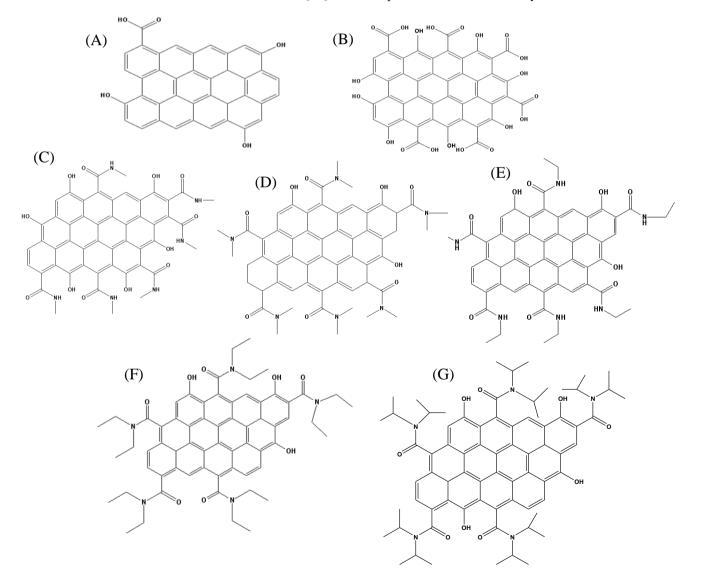

Figure 1. Schematic representation of (A) AC, (B) ON, (C) ONM, (D) ONDM, (E) ONE, (F) ONDE, and (G) ONDIP [24].

As the size of alkylamine increases, the functionalization decreases due to steric effects [24]. These seven carbons were tested for MB adsorption in this study.

3.1 Effect of pH on methylene blue adsorption

The adsorption of MB depends on the pH of the aqueous solution. The amount of MB adsorbed was calculated from Equation 1.

$$q_e = (C_o - C_e)V/m \qquad \text{Eq. (1)}$$

where q_e is MB adsorbed (mg/g) at equilibrium, C_o, and C_e are initial and equilibrium MB concentration (mg/L), V is the volume in L, and m is the mass of adsorbent (g). As MB is a cationic dye regardless of the pH of the solution, the variation of MB adsorption with initial pH is mostly related to the surface properties at different pH values. As shown in Figure 2A, MB adsorption remains almost constant for AC, ONM, ONDM, ONE, and ONDIP regardless of the initial pH values. However, for ON and ONDE, a slight decrease at low pH was observed. The insignificant variation of MB adsorption onto ONM, ONDM, ONE, and ONDIP is related to the dominance of hydrophobic interaction forces between the hydrophobic surface and MB. However, MB adsorption onto AC is dominated by van der Waals' interaction forces, and $\pi-\pi$ interactions [25]. MB adsorption onto ON (pH_{zpc} 3.38 [24]) shows low adsorption at pH 3. At this pH, the surface is protonated and neutral. However at higher pH, adsorption increases and remains constant in the range of pH 7-9. In that range of pH, electrostatic interaction between the negatively charged ON surface and MB cations dominate the adsorption process. Thus, pH 7.0 was selected for further studies. ONE and ONDIP show higher MB adsorption than AC or ON. ONDE shows less adsorption due to the limited extent of functionalization, self-adsorption, and entangling of immobilized diethylamine chains [24]. The final pH against the initial pH is presented in Figure 2B. There is a slight increase in the final pH in the acidic range and this could be due to the protonation of unfunctionalized carboxylic groups. The final pH seems to be less than the initial pH in the alkaline initial pH range and this could be due to OH⁻ adsorption onto adsorbed MB molecules as a second layer.
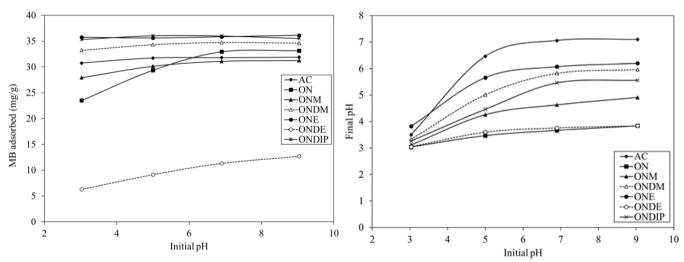

Figure 2. (A) Effect of pH on MB adsorption, (B) Initial pH vs final pH for MB adsorption.

3.2 Kinetics of MB adsorption

The kinetics of MB adsorption is presented in Figure 3. At 20 °C, approximate equilibrium was reached within 35 hours for AC and ON, and ~ 24 hours for hydrophobic activated carbons. At 40 °C, the equilibrium time was reached faster for ONDIP, ONDE (12 hours), and AC and ON (24 hours). MB adsorption was enhanced with the temperature rise. MB adsorption was found to vary almost linearly with the half power of time, in the initial stage of adsorption. This was observed by applying the pore diffusion model [26] (Equation 2).

$$q_t = k_d t^{0.5} \qquad \text{Eq. (2)}$$

where q_t is MB adsorbed at time t and k_d is the pore diffusion constant (mg/g/ $h^{0.5}$). As the temperature increases, k_d values increase for all carbons investigated (Table 1). k_d (mg/g/hr$^{0.5}$) follows the order of ONDIP> ONE > ONDM > ON>ONM> AC > ONDE at 20 °C. The same order is followed at 40 °C except for ONM, which is slightly higher than ON.
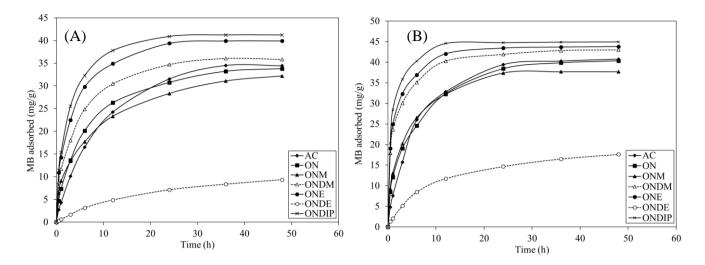
Figure 3. Kinetics of MB adsorption at (A) 20 $^{\circ}$C and (B) 40 $^{\circ}$C.

MB adsorption kinetic data were investigated for pseudo-first-order and pseudo-second-order kinetic models (Equations 3 & 4).

$$log(q_e\text{-}q_t) = log\ q_e - k_1t/2.303 \qquad \text{Eq. (3)}$$

$$t/q_t = 1/k_2qe^2 + t/q_e \qquad \text{Eq. (4)}$$

Where k_1 and k_2 are pseudo-first-order rate constant (hr^{-1}), and pseudo-second-order constant (g/mg/hr). The initial adsorption rate can be obtained from Equation 5.

$$h = k_2q_e^2 \qquad \text{Eq. (5)}$$

The plots of log ($q_e - q_t$) versus t show straight lines from which q_e and k_1 are determined. The linear plots of the pseudo-first-order model for MB adsorption show low correlation values (R^2) indicating poor fit to the model, Table 1, and thus, the kinetic parameters of this model are not discussed. The linear plots of t/q_t versus t for the pseudo-second-order kinetic model show straight lines with high correlation values (R^2), Table 1. Such good fit suggests that the adsorption of MB complies very well with the pseudo-second-order kinetic reaction between MB and the carbons' surfaces. This reflects that the rate of MB adsorption depends on both the adsorbent and adsorbate and the limiting step in the adsorption process involves sharing or exchange of electrons between the carbon surface and MB [27,28]. q_e, h, and k_2 values from the pseudo-second-order model are found to increase with temperature increase similarly to k_d increase. The rise in temperature decreases the solvation layers around the adsorbent and adsorbate allowing faster diffusion and more access to active sites and consequently more MB uptake [29,30]. k_2, h and q_e follow the order of ONDIP> ONE > ONDM > ON ≈ ONM> AC > ONDE. AC shows fewer values of the rate constants because MB molecules diffuse through a network of porous structures within AC particles. ONDIP, ONE, ONDM, and ONM show faster adsorption than AC because the active sites here are externally immobilized chains. ONDIP and ONE show higher kinetic parameters of k_d, k_2, and h. ONDE shows the slowest MB adsorption due to the self-adsorption or entangling of immobilized chains [24]. ON shows a faster kinetic process than AC and this is related to a different mechanism of electrostatic interaction involved between the negatively charged ON and the positively charged MB.

The activation energies, E_a (kJ/mol) for MB adsorption were calculated considering the rate constant (k_2) due to the good fit to the pseudo-second-order model. The energy of activation, E_a, was calculated from the Arrhenius equation for two temperatures (Equation 6).

$$\ln(\frac{k_2^{'}}{k_2}) = \frac{E_a}{R}(\frac{1}{T_1} - \frac{1}{T_2}) \qquad \text{Eq. (6)}$$

R is the gas constant (8.314 J mol^{-1} K^{-1}), k_2 is the rate constant at T$_1$ (298 K) and k'_2 is the rate constant at T$_2$ (213 K). The lower values of E_a indicate physical adsorption processes (E_a <42 kJ/mol), whereas higher values of E_a (E_a > 42 kJ/mol) indicate chemically controlled processes [30]. The E_a values for MB adsorption lie between 5.85 and 36.12 kJ/mol (Table 1) indicating physisorption domination.

Table 1. Kinetic parameters of MB adsorption on AC, ON, and ON hydrophobic carbons at 20 and 40 ^{o}C.

Sorbent	Temp.	Pore diffusion constant, k_d (mg/g h$^{0.5}$)	Pseudo-first-order model			Pseudo-second-order model				E_a, (kJ/mol)
			k_1 (h^{-1})	q_e (mg/g)	R^2	rate const. k_2, (g/mg/h)	Initial adsorption rate, h, (mg/g/h)	q_e, (mg/g)	R^2	
AC	20 ^{o}C	5.34	0.081	4.29	0.9560	0.0029	4.99	41.32	0.9969	5.85
	40 ^{o}C	9.53	0.169	6.12	0.8609	0.0034	8.10	43.78	0.9972	
ON	20 ^{o}C	9.28	0.149	4.96	0.9211	0.0061	8.25	36.90	0.9989	6.06
	40 ^{o}C	12.17	0.158	5.15	0.9367	0.0711	13.21	43.10	0.9979	
ONM	20 ^{o}C	8.90	0.107	4.40	0.9520	0.0069	8.22	34.48	0.9944	16.43
	40 ^{o}C	12.90	0.104	4.26	0.9645	0.0106	16.89	39.84	0.9989	
ONDM	20 ^{o}C	10.1	0.104	3.88	0.9153	0.0102	14.71	38.02	0.9988	26.47
	40 ^{o}C	19.54	0.118	3.27	0.9512	0.0204	39.53	44.05	0.9998	
ONE	20 ^{o}C	11.49	0.191	4.56	0.9611	0.0116	20.33	41.84	0.9994	28.81
	40 ^{o}C	20.01	0.098	3.60	0.9325	0.0247	49.26	44.64	0.9999	
ONDE	20 ^{o}C	0.95	0.094	2.93	0.8906	0.0039	0.662	13.09	0.9985	14.11
	40 ^{o}C	2.51	0.137	3.75	0.9910	0.0056	2.37	20.58	0.9984	
ONDIP	20 ^{o}C	13.63	0.139	3.85	0.9532	0.0137	25.19	42.92	0.9997	36.12
	40 ^{o}C	27.45	0.126	2.78	0.8709	0.0353	73.53	45.66	0.9999	

3.3 Equilibrium studies and temperature effect

MB adsorption follows an L-type adsorption isotherm with better performance as the temperature rises (Figure 4). MB uptake increases with the increase in dye concentration reaching a plateau at high MB concentrations. The concentration of the dye acts as a driving force to overcome mass transfer resistance for the transport of dye molecules from the aqueous solution to the carbon surface. When the surface is saturated with the dye molecules, available active sites decrease, obstructing further uptake of the dye molecules and reaching a plateau [31]. The increased MB adsorption is related to the desolvation of the carbon particles and dye molecules by temperature rise allowing more access to active sites and consequently, more MB uptake [29,30].
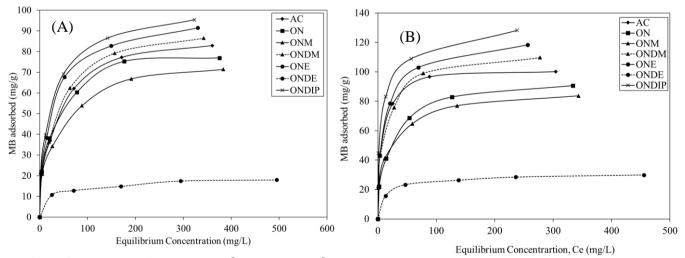

Figure 4. Adsorption of MB at (A) 20 ^{o}C and (B) at 40 ^{o}C (initial pH 7).

The adsorption isotherms are used to characterize the adsorption systems. Despite the availability of different isotherm equations, the most commonly used isotherms are the Langmuir and Freundlich isotherms (Equations 7 and 8), respectively.

$$C_e/q_e = 1/b.q + C_e/q \qquad \text{Eq. (7)}$$
$$\log q_e = \log K + (1/n) \log C_e \qquad \text{Eq. (8)}$$

where q is the monolayer capacity (mg/g), and b is the Langmuir constant (L/mg). K (l$^{1/n}$ mg$^{1-1/n}$ /g) and $1/n$ are the Freundlich constants, which are relative indicators of adsorption capacity and adsorption intensity, respectively.

The Langmuir isotherm model assumes the formation of monolayer coverage of adsorbates at equilibrium as adsorption sites become occupied by the adsorbate, after which no adsorption can take place at the occupied sites [32]. In contrast, for surfaces having non-uniform energy distribution, the Freundlich isotherm is extensively used [33]. Adsorption data were found to fit the Langmuir model well with high values of R^2 (Table 2). On the other hand, the adsorption data do not show good fit to the Freundlich model showing low correlation values of R^2 (Table 2). MB adsorption favors monolayer formation at equilibrium following the Langmuir adsorption model well.

The adsorption capacity (q) of MB increased with the rise in temperature for all carbons tested. This could be due to the desolvation of dyes and the decrease in the thickness of boundary aqueous layers of carbons and MB molecules with temperature rise [29,30]. As a result, the mass transfer resistance of dye in the boundary layer decreases. q follows the order of ONDIP > ONE > ONDM > AC > ON > ONM > ONDE. ONDIP, ONE, and ONDM are hydrophobic activated carbons with incomplete surface functionalization due to the large size of the alkylamine immobilized. The unfunctionalized content of carboxylic groups acts as a barrier between the immobilized hydrophobic chains disallowing hydrophobic interaction between the immobilized chains or their entangling together [24]. This allows more interaction of MB molecules with the hydrophobic active sites and thus enhanced MB uptake. On the other hand for ONM, surface functionalization extent is high and this provides small hydrophobic active sites (methyl group). Thus, the large MB molecules can be adsorbed onto multiple active sites simultaneously. This restricts further access to the inner surface active sites and, thus, MB adsorption decreases. For ONDE, the long diethyl chains immobilized are probably self-adsorbed onto the carbon surface [24] or entangled with adjacent diethyl chains minimizing the uptake of MB dye. For AC, despite having a large surface area (588 m²/g), it shows less adsorption of MB compared with ONDIP, ONE, and ONDM which possess lower surface area. It is expected that the immobilized hydrophobic chains onto ONDIP, ONE, and ONDM can adsorb multiple molecules of MB. MB adsorption onto AC takes place mostly via van der Waals forces and π-π interactions [19, 34, 35].

Table 2. Equilibrium parameters for MB adsorption at different temperatures.

Sorbent	Sorption Temp. °C	Langmuir constants		Separation factor, R_s	R^2	Freundlich constants		R^2
		q (mg/g)	b (L/mg)			$1/n$	K	
AC	20 °C	88.5	0.040	0.04-0.33	0.9983	0.333	13.2	0.9719
	40 °C	102.0	0.153	0.01-0.12	0.9999	0.288	24.2	0.8388
ON	20 °C	81.3	0.052	0.03-0.28	0.9983	0.298	15.0	0.9681
	40 °C	94.3	0.064	0.03-0.24	0.9985	0.367	40.7	0.9698
ONM	20 °C	75.8	0.038	0.05- 0.35	0.9970	0.303	12.9	0.9838
	40 °C	86.2	0.075	0.02-0.21	0.9986	0.270	19.5	0.9678
ONDM	20 °C	91.8	0.044	0.04-0.32	0.9968	0.318	14.9	0.9796
	40 °C	112.4	0.129	0.01-0.14	0.9985	0.302	24.2	0.9328
ONE	20 °C	96.2	0.055	0.03-0.27	0.9981	0.314	16.73	0.9707
	40 °C	122.0	0.117	0.02-0.15	0.9990	0.308	25.8	0.9371
ONDE	20 °C	19.04	0.032	0.06-0.38	0.9970	0.180	1.20	0.986
	40 °C	30.86	0.058	0.03-0.26	0.9994	0.180	10.6	0.9277
ONDIP	20 °C	99.0	0.061	0.03-0.25	0.9981	0.308	18.14	0.9748
	40 °C	131.6	0.158	0.01-0.11	0.9988	0.283	32.2	0.8543

ON shows less MB adsorption than AC and this is probably related to the incomplete saturation of the ON surface by the MB molecule due to its larger size.

Another characteristic of the Langmuir isotherm is the separation factor, R_s, (Equation 9).

$$R_s = 1/(1+bC_o)$$
Eq. (9)

The effectiveness of the adsorption process can be predicted from the values of the separation factor. For $R_s = 0$, the adsorption is irreversible, and when R_s lies between 0 and 1, the adsorption is favorable [36]. If R_s is larger than 1, the adsorption is unfavorable but if $R_s = 1$, the adsorption is linear [36]. Table 2 shows that R_s is between 0 and 1 indicating that the adsorption of MB is favorable. As the values of R_s approach zero, this indicates strong adsorption tending to irreversibility.

The monolayer adsorption capacity of MB on adsorbents, in this study, can be compared with different adsorbents in other studies. For AC, prepared by phosphoric acid activation from coconut shell, MB capacity was 200 mg/g [37]. Other adsorbents showed different capacities including AC prepared by potassium hydroxide activation (270 mg/g) [19], dehydrated carbon (196.1 mg/g) [20], ethylamine hydrophobic activated carbon (393 m²/g), lignin (34 mg/g) [38], D-fructose (83 mg/g) [39], and anaerobic activated sludge (91 mg/g) [40]. In another study, AC showed a

capacity of 127.6 mg/g; however, on modification with sodium lauryl sulfate the capacity increased to 195.7 mg/g [2]. In this study, AC and ONDIP show adsorption capacities of 131.6 and 102 mg/g of MB, respectively.

3.5 Thermodynamic parameters

The thermodynamic parameters were calculated for the adsorption of MB onto the carbons under investigation. The parameters were calculated from the change in equilibrium constant, K_c, at 20 and 40°C. K_c can be calculated using Equation 10.

$$K_c = C_{Ae}/ C_e \qquad \text{Eq.(10)}$$

where C_{Ae} is the amount of MB adsorbed (mg) per liter of solution, and C_e is the equilibrium concentration of MB solution (mg/L). K_c is estimated from the initial part of the adsorption isotherm where q_e versus C_e is linear. The Gibbs free energy change of the adsorption ($\Delta G°$), is related to K_c as shown in Equation 11 [41].

$$\Delta G^o = -RTlnK_c \qquad \text{Eq. (11)}$$

where R is the gas constant (8.314 J mol^{-1} K^{-1}) and T is the absolute temperature (K). The enthalpy (ΔH^o) can be calculated from the Van't Hoff equation (Equation 12) [41].

$$\ln(\frac{k_{c2}}{k_{c1}}) = \frac{\Delta H^o}{R}(\frac{1}{T_1} - \frac{1}{T_2}) \qquad \text{Eq. (12)}$$

where k_{c1} and k_{c2} are the equilibrium constants at T_1 and T_2, respectively. From ΔG^o and ΔH^o, the entropy change, ΔS^o, is calculated from Equation 13.

$$\Delta G^o = \Delta H^o - T\Delta S^o \qquad \text{Eq. (13)}$$

Thermodynamic parameters for the adsorption of MB are shown in Table 3. K_c values increase with temperature indicating an endothermic nature of MB adsorption [41]. The negative values of ΔG^o indicate spontaneous adsorption processes, which is usually the case for the adsorption of organic compounds from solution [42]. In addition, ΔG^o values decrease further with the increase in temperature indicating that higher temperature enhances MB adsorption. ONDE shows a positive ΔG^o at 20 °C, indicating a nonspontaneous process at this temperature.

Table 3. Thermodynamic parameters of MB adsorption on different carbons.

Carbon	Temp.(K)	K_c	ΔG^o (kJ/mol)	ΔH^o (kJ/mol)	ΔS^o (J/mol)
AC	293	9.07	-5.37	34.95	137.6
	313	22.68	-8.12		
ON	293	10.39	-5.70	27.05	111.8
	313	21.11	-7.94		
ONM	293	8.43	-5.19	36.90	143.3
	313	22.20	-8.07		
ONDM	293	15.19	-6.63	34.78	146.3
	313	37.83	-9.45		
ONE	293	18.43	-7.10	35.75	143.8
	313	47.09	-10.02		
ONDE	293	0.96	0.09	38.46	131.0
	313	2.64	-2.53		
ONDIP	293	21.63	-7.49	31.55	133.3
	313	49.49	-10.15		

The positive values of ΔH^o thermodynamically indicate an endothermic nature of MB adsorption. ΔH^o values are less than 40 kJ/mol, indicating the physical adsorption nature of the MB. ΔH^o values higher than 40 kJ/mol represent chemisorption processes [43]. The adsorption of methylene blue on AC showed an endothermic spontaneous process [43]. The positive value of ΔS^o reveals an increase in the degree of randomness for all tested carbons at the solid-solution interface for MB adsorption. Previous studies showed similar trends for MB adsorption [43-45].

3.6 Reuse of adsorbents for dye adsorption

AC, ONDM, ONE, and ONDIP were selected for this study (Figure 5). AC shows less uptake in the second adsorption cycle showing 79 % uptake compared with the first adsorption cycle. It is known that AC has limited reuse because it is difficult to desorb the adsorbate molecules from deep locations inside the porous structure [41]. On the other hand, ONDIM, ONE, and ONDIP reached 98.6, 99.5, and 99.6 % of MB adsorption in the second adsorption cycle compared with the first adsorption cycle.
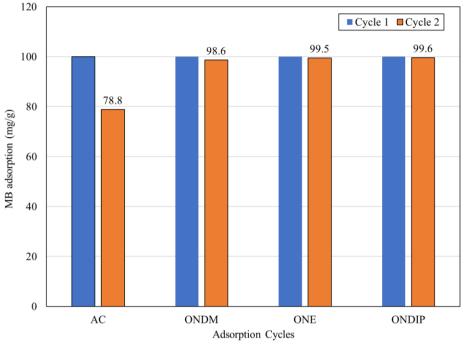

Figure 5. Carbon reuse for MB adsorption.

4. Conclusion

AC, ON, and ON functionalized with different alkylamines (ONM, ONDM, ONE, ONDE, and ONDIP) were tested for MB adsorption. pH 7 was found to be optimum for MB adsorption. MB adsorption follows a pseudo-second-order kinetic model with the rate of adsorption increasing with temperature rise. The activation energy, E_a, was found to be less than 42 kJ/mol indicating physical adsorption and diffusion-controlled processes. Equilibrium adsorption follows L-type isotherms with the adsorption data fitting well with the Langmuir model, and better than with the Freundlich model. The adsorption capacity (q) was enhanced with temperature rise. The adsorption for MB follows the order of ONDIP > ONE > ONDM > AC > ON > ONM > ONDE. The thermodynamic parameters show that the dye adsorption is endothermic and spontaneous. ONDIP, ONE, and ONDM show faster MB uptake, more adsorption, and better recycling properties than AC.

Conflict of interest

The authors declare no conflict of interest.

References

1. Pearce, C.I., Lloyd, J.R., Guthrie, J.T. The removal of colour from textile wastewater using whole bacterial cells: a review. *Journal of Dyes and Pigments*, 2003, **58**, 179-196.
2. Kuang, Y., Zhang, X., Zhou, S. Adsorption of methylene blue in water onto activated carbon by surfactant modification. *Water*, 2020, **12**, 587.
3. Forgacs, E., Cserhati, T., Oros, G. Removal of synthetic dyes from wastewater: A review. *Journal of Environment International*, 2004, **30**, 953-971.

4. Ravikumar, K., Ramalingam, S., Krishnan, S., Balu, K. Application of response surface methodology to optimize the process variables for reactive red and acid brown dye removal using a novel adsorbent. *Journal of Dyes and Pigments*, 2006, **70**, 18-26.

5. Zhang, Y., Zhang, S., Gao, J., Chung, T.S. Layer-by-layer construction of graphene oxide (GO) framework composite membranes for highly efficient heavy metal removal. *Journal of Membrane Science*, 2016, **515**, 230-237.

6. Akodad, M., Baghour, M., Moumen, A., Skalli, A., Azizi, G., Anjjar, A., Aalaoul, M., Daoudi, I. Adsorption of a basic dye, Methylene Blue, in aqueous solution on bentonite. *Moroccan Journal of Chemistry*, 2021, **9**, 416 - 433.

7. Asgher, M., Bhatti, H. N., 2012. Evaluation of thermodynamics and effect of chemical treatments on sorption potential of (Citrus) waste biomass for removal of anionic dyes from aqueous solutions. *Journal of Ecological Engineering*, 2012, **38**, 79-85.

8. Kadirvelu, K., Kavipriya, M., Karthika, C., Radhika, M., Vennilamani, N., Pattabhi, S. Utilization of various agriculture wastes for activated carbon preparation and application for the removal of dyes and metal ions from aqueous solutions. *Journal of Bioresource Technology*, 2003, **87**, 129-132.

9. Liu, H., Yu, J., Liu, X. Study on the ozonation degradation of methylene blue enhanced by microchannel and ultrasound. *Water Science and Technology*, 2023, **87**, 598-613.

10. Chahar, D., Kumar, D., Thakur, P., Thakur, A. Visible light induced photocatalytic degradation of methylene blue dye by using Mg doped Co-Zn nanoferrites. *Materials Research Bulletin*, 2023, **162**, 112205.

11. Raizada, P., Sudhaik, A., Singh, P., 2019. Photocatalytic water decontamination using graphene and ZnO coupled photocatalysts: A review. *Materials Science for Energy Technologies*, 2019, **2**, 509-525.

12. Asghar, A., Abdul Raman, A.A., Wan Daud, W.M.A. Advanced oxidation processes for in-situ production of hydrogen peroxide/hydroxyl radical for textile wastewater treatment: A review. *Journal of cleaner production*, 2015, **87**, 826-838.

13. Hedaoo, M.N., Bhole, A.G., Ingole, N.W., Hung, Y.T. Biological wastewater treatment". In *Handbook of environment and waste management: Air and water pollution control* (1st edition), World Scientific, London, 2012.

14. Verma, A.K., Dash, R.R., Bhunia, P. A review on chemical coagulation/flocculation technologies for removal of color from textile wastewaters. *Journal of Environmental Management*, 2012, **93**, 154-168.

15. Alventosa-deLara, E., Barredo-Damas, S., Alcaina-Miranda, M.I., Iborra-Clar, M.I. Ultrafiltration technology with a ceramic membrane for reactive dye removal: Optimization of membrane performance. *Journal of Hazardous Materials*, 2012, **209–210**, 492–500.

16. Yagub, M.T., Sen, T.K., Afroze, S., Ang, H.M. Dye and its removal from aqueous solution by adsorption: A review. *Advances in Colloid and Interface Science*, 2014, **209**, 172-184.

17. Karaca, S., Gürses, A., Açıkyıldız, M., Ejder, M.K. Adsorption of cationic dye from aqueous solutions by activated carbon. *Microporous and Mesoporous Materials*, 2008, **115**, 376-382.

18. Dolas, H. Activated carbon synthesis and methylene blue adsorption from pepper stem using microwave assisted impregnation method: Isotherm and kinetics. *Journal of King Saud University-Science*, 2023, **35**, 102559.

19. El-Shafey, E.I., Ali, S.N., Al-Busafi, S., Al-Lawati, H.A. Preparation and characterization of surface functionalized activated carbons from date palm leaflets and application for methylene blue removal. *Journal of Environmental Chemical Engineering*, 2016, **4**, 2713-2724.

20. El-Shafey, E.I., Ali, S.N., Al-Lawati, H., Al-Busafi, S. Preparation and characterization of acidic, basic and hydrophobic dehydrated carbons and their capability for methylene blue adsorption. *Sultan Qaboos University Journal for Science [SQUJS]*, 2019, **24**, 23-35.

21. Allaoui, S., Bennani, M.N., Ziyat, H., Qabaqous, O., Tijani, N., Ittobane, N. Removing polyphenols contained in olive mill wastewater by membrane based on natural clay and Hydrotalcite Mg-Al. *Moroccan Journal of Chemistry*, 2020, **8**, 318-325.

22. Alver, E., Metin, A.Ü. Anionic dye removal from aqueous solutions using modified zeolite: Adsorption kinetics and isotherm studies. *Chemical Engineering Journal*, 2012, **200**, 59-67.

23. Silva, F., Nascimento, L., Brito, M., da Silva, K., Paschoal Jr, W., Fujiyama, R. Biosorption of methylene blue dye using natural biosorbents made from weeds. *Materials*, 2019, **12**, 2486.

24. El-Shafey, E.I., Al-Mashaikhi, S.M., Al-Busafi, S., Suliman, F.O. Effect of alkylamine immobilization level on the performance of hydrophobic activated carbon. *Materials Chemistry and Physics*, 2022, **286**, 126154.

25. Muzarpar, M.S., Leman, A.M., Rahman, K.A., Maghpor, N., Hassana, N.N.M., Misdan, N. the adsorption mechanism of activated carbon and its application-A review. *International Journal of Advanced Technology in Mechanical, Mechatronics and Materials*, 2020, **1**, 118-124.

26. Weber Jr, W.J., Morris, J.C. Kinetics of adsorption on carbon from solution. *Journal of the Sanitary Engineering Division*, 1963, **89,** 31-59.

27. Ho, Y.-S., McKay, G. Pseudo-second order model for sorption processes. *Process Biochemistry,* 1999, **34,** 451-465.

28. Ho, Y.-S. Review of second-order models for adsorption systems. *Journal of Hazardous Materials*, 2006, **136,** 681-689.

29. El-Shafey, E.S.I., Al-Lawati, H.A., Al-Hussaini, A.Y. Adsorption of fexofenadine and diphenhydramine on dehydrated and activated carbons from date palm leaflets. *Chemistry and Ecology*, 2014, **30**, 765-783.

30. Liu, C., Huang, P.M. Kinetics of lead adsorption by iron oxides formed under the influence of citrate. *Geochimica et Cosmochimica Acta*, 2003, **67**, 1045-1054.

31. Duran, C., Ozdes, D., Gundogdu, A., Senturk, H.B.. Kinetics and isotherm analysis of basic dyes adsorption onto almond shell (Prunus dulcis) as a low cost adsorbent. *Journal of Chemical & Engineering Data*, 2011, **56**, 2136-2147.

32. Langmuir, I. The adsorption of gases on plane surfaces of glass, mica and platinum. *Journal of the American Chemical Society*, 1918, **40**, 1361-1403.

33. Freundlich, H.M.F. Constitution and fundamental properties of solids and liquids I. *Solids. Journal of Physical Chemistry A*, 1960, **57**, 385-470.

34. Han, Q., Wang, J., Goodman, B.A., Xie, J., Liu, Z. High adsorption of methylene blue by activated carbon prepared from phosphoric acid treated eucalyptus residue. *Powder Technology*, 2020, **366**, 239-248.

35. Xue, H., Wang, X., Xu, Q., Dhaouadi, F., Sellaoui, L., Seliem, M.K., Lamine, A.B., Belmabrouk, H., Bajahzar, A., Bonilla-Petriciolet, A., Li, Z. Adsorption of methylene blue from aqueous solution on activated carbons and composite prepared from an agricultural waste biomass: A comparative study by experimental and advanced modeling analysis. *Chemical Engineering Journal*, 2022, **430**, 132801.

36. Hall, K.R., Eagleton, L.C., Acrivos, A., Vermeulen, T. Pore-and solid-diffusion kinetics in fixed-bed adsorption under constant-pattern conditions. *Industrial & Engineering Chemistry Fundamentals*, 1966, **5**, 212-223.

37. Islam, M.A., Ahmed, M.J., Khanday, W.A., Asif, M., Hameed, B.H. Mesoporous activated coconut shell-derived hydrochar prepared via hydrothermal carbonization-NaOH activation for methylene blue adsorption. *Journal of Environmental Management*, 2017, **203**, 237-244.

38. Albadarin, A.B., Collins, M.N., Naushad, M., Shirazian, S., Walker, G., Mangwandi, C. Activated lignin-chitosan extruded blends for efficient adsorption of methylene blue. *Chemical Engineering Journal*, 2017, **307**, 264-272.

39. Alatalo, S.M., Mäkilä, E., Repo, E., Heinonen, M., Salonen, J., Kukk, E., Sillanpää, M., Titirici, M.M. Meso-and microporous soft templated hydrothermal carbons for dye removal from water. *Green Chemistry*, 2016, **18**, 1137-1146.

40. Shi, L., Zhang, G., Wei, D., Yan, T., Xue, X., Shi, S., Wei, Q. Preparation and utilization of anaerobic granular sludge-based biochar for the adsorption of methylene blue from aqueous solutions. *Journal of Molecular Liquids*, 2014, **198**, 334-340.

41. Ali, S.N., El-Shafey, E.I., Al-Busafi, S., Al-Lawati, H.A. Adsorption of chlorpheniramine and ibuprofen on surface functionalized activated carbons from deionized water and spiked hospital wastewater. *Journal of Environmental Chemical Engineering*, 2019, **7**, 102860.

42. Wu, Z., H. Joo, K. Lee, Kinetics and thermodynamics of the organic dye adsorption on the mesoporous hybrid xerogel. *Chemical Engineering Journal*, 2005, **112,** 227-236.

43. Li, H., Liu, L., Cui, J., Cui, J., Wang, F., Zhang, F. High-efficiency adsorption and regeneration of methylene blue and aniline onto activated carbon from waste edible fungus residue and its possible mechanism. *RSC Advances*, 2020, **10**, 14262-14273.

44. Yadav, S., Tyagi, D.K. and Yadav, O.P. Equilibrium and kinetic studies on adsorption of aniline blue from aqueous solution onto rice husk carbon. *International Journal of Chemistry Research*, 2011, **2**, 59-64.

45. Okasha, A., Ghoneim, H.S., Khalil, E. and Mohamed, S.. Kinetics and thermodynamics of aniline blue adsorption onto cross-linked gelatin/chitosan polymer blends. *Journal of Textiles, Coloration and Polymer Science*, 2019, **16**, 113-127.